

ORIGINAL ARTICLE

Intermittent and continuous imatinib in a human GIST xenograft model carrying *KIT* exon 17 resistance mutation D816HMONA-ELISABETH REVHEIM^{1,2}, ALEXANDR KRISTIAN^{2,3}, EIRIK MALINEN⁴, ØYVIND SVERRE BRULAND^{2,5}, JEANNE-MARIE BERNER⁶, RUTH HOLM⁶, HEIKKI JOENSUU⁷ & THERESE SEIERSTAD^{1,8}

¹Department of Radiology and Nuclear Medicine, Oslo University Hospital, Nydalen, Oslo, Norway, ²Institute of Clinical Medicine, University of Oslo, Blindern, Oslo, Norway, ³Institute for Cancer Research, Oslo University Hospital, Nydalen, Oslo, Norway, ⁴Department of Medical Physics, Oslo University Hospital, Nydalen, Oslo, Norway, ⁵Department of Oncology, Oslo University Hospital, Nydalen, Oslo, Norway, ⁶Department of Pathology, Oslo University Hospital, Nydalen, Oslo, Norway, ⁷Department of Oncology, Helsinki University Central Hospital, Helsinki, Finland and ⁸Faculty of Health Sciences, Buskerud University College, Drammen, Norway

Abstract

Background. Acquired resistance to imatinib is frequently caused by secondary *KIT* mutations. We have investigated the effects of imatinib in mice with human gastrointestinal stromal tumour (GIST) xenograft which harbours a primary exon 11 deletion mutation and a secondary imatinib resistance mutation D816H in exon 17. Such mutations are commonly present in imatinib-resistant GIST in humans. **Material and methods.** The mice were randomly allocated to receive imatinib either continuously or intermittently. Dynamic ¹⁸F-FDG PET was performed and blood volume fraction (v_B), rate transfer constants (k_1 , k_2 , k_3) and metabolic rate of ¹⁸F-FDG (MR_{FDG}) were computed using a three-compartment model. Tumours were evaluated for the mitotic rate and the expression of HIF-1 α , caspase-3 and glucose transporters (GLUTs). **Results.** Both intermittent and continuous imatinib delayed tumour growth significantly compared to controls, significantly in favour of the latter. k_1 (representing perfusion, vascular permeability and binding of ¹⁸F-FDG to the GLUTs) was significantly higher in the intermittent group compared to the continuous group, as was tumour GLUT-3 expression. k_3 (representing internalisation of ¹⁸F-FDG to the cells) and MR_{FDG} were significantly lower. **Conclusion.** Imatinib delays GIST xenograft growth despite the presence of the D816H resistance mutation. The schedule of imatinib administration may influence tumour glucose uptake rate and metabolic rate.

Gastrointestinal stromal tumour (GIST) is the most common sarcoma of the digestive tract [1]. Approximately 95% of GISTs express *KIT*, the receptor for the stem cell factor [2]. *KIT* mutations frequently result in *KIT* phosphorylation and constitutive activation. In a few GISTs (5–10%) a mutation is found in the gene encoding the platelet-derived growth factor receptor alpha (*PDGFRA*). Both *KIT* and *PDGFRA* receptors are tyrosine kinases and key players in GIST tumorigenesis [3]. By the introduction of the tyrosine kinase inhibitor (TKI) imatinib, a selective inhibitor of *KIT*, *PDGFRA* and a few other kinases, a new era in the management of GIST began

[4,5]. Most patients with advanced GIST respond to imatinib, the standard first-line treatment, but the majority eventually progress with the median time to imatinib resistance being approximately two years [5]. In acquired imatinib resistance secondary mutations in *KIT* exons 13 and 17 are common resulting in a kinase conformation that prohibits imatinib from binding to the kinase [6].

A metabolic response to imatinib in GIST may be observed early with 2-deoxy-2-[¹⁸F]fluoro-D-glucose (¹⁸F-FDG) positron emission tomography (PET) [4], sometimes even within a few hours after starting imatinib [7,8]. Dynamic ¹⁸F-FDG PET

enables assessment of tissue uptake of the tracer in space and time following injection and may offer valuable information about tumour vascularisation and its metabolic characteristics [9].

Human tumour xenografts are useful for evaluating novel therapeutic agents, since tumour vascular and stromal components cannot be addressed *in vitro*. The GIST human xenograft model AHAX [10] originates from a patient with a clinically imatinib-resistant GIST harbouring a primary *KIT* exon 11 mutation (sensitive to imatinib) and a secondary *KIT* exon 17 mutation (likely treatment-induced mutation). Since *KIT* exon 11 is the most common site of mutation in primary GIST and *KIT* exon 17 is the most frequent site of a secondary resistance mutation [11], this model reflects the most common clinical scenario in imatinib-resistant GIST.

Imatinib, administered usually continuously at a dose of 400 mg/day, is generally well tolerated and despite prior tumour progression during first-line imatinib it is often considered as the last-line palliative systemic treatment for patients with advanced GIST [12]. This practice is, however, controversial in the absence of other than anecdotal supportive clinical experiences. A randomised clinical trial is currently comparing imatinib plus the best supportive care to the latter alone as palliative treatment of advanced GIST (ClinicalTrials.gov identifier NCT1151852). Somewhat unexpectedly withdrawal of imatinib in responding patients and reinstitution of imatinib at the time of metastatic progression, did not affect survival in a large randomised clinical trial [13,14].

The aim of the present study was to evaluate the potential benefits of continuous and intermittent imatinib administration in an experimental human GIST xenograft model harbouring imatinib resistance mutation. This was evaluated by tumour growth measurements and assessment of tumour metabolic activity (with dynamic ^{18}F -FDG PET), mitotic rate, and expression of HIF-1 α , caspase-3 and GLUTs.

Material and methods

Animals and xenografts

Human GIST AHAX xenografts with a mutation in *KIT* exon 11 (c.1673_1687del, p.Lys558_Glu562del) and *KIT* exon 17 (c.2446G> C, p.Asp816His) [10] were established by subcutaneous implantation of tumour tissue fragments ($\sim 2 \times 2 \times 2 \text{ mm}^3$) bilaterally into NCR athymic mice. The mice were kept under specific pathogen-free conditions at a constant temperature (22–24°C) and humidity (55–60%), and were given sterilised food and tap water ad libitum.

Six weeks after implantation 37 mice were randomly allocated into a control group (n = 12) or to one of two imatinib treatment groups, where imatinib

was administered either continuously (n = 13) or intermittently (n = 12, one week on and one week off). The study was approved by the Institutional Committee on Research on Animal Care and was performed according to Interdisciplinary Principles and Guidelines for the Use of Animals in Research, Marketing and Education (New York Academy of Science, New York, NY, USA).

Tumour volume measurements

Tumour size was measured by a caliper twice weekly from the date of implantation. Tumour volume was calculated using the modified ellipsoid formula [15], where the volume $V(\text{mm}^3) = (\pi/6) \times a(\text{mm}) \times b^2(\text{mm}^2)$, a and b being the longest and the perpendicular tumour diameters, respectively. The measurements were normalised to individual pre-treatment (day 0) tumour volumes. Estimated tumour volume doubling time was calculated using linear regression on ln-transformed normalised tumour volumes.

Imatinib administration

Imatinib (Glivec[®], Novartis Pharma GmbH, Basel, Switzerland) was dissolved in distilled water and given by oral gavage: either 100 mg/kg once daily (the continuous treatment group) or in two-week cycles, with imatinib given daily for seven days followed by placebo (water) for seven days (the intermittent treatment group). The control group received water only by oral gavage. The duration of the experiment was 91 days.

Dynamic ^{18}F -FDG PET imaging

Four mice from each of the three groups underwent dynamic ^{18}F -FDG PET one day prior to sacrifice, using a small animal PET scanner (microPET Focus 120, Siemens Medical Solutions, Erlangen, Germany). Following overnight fasting the mice were anaesthetised and given an *i.v.* bolus injection of 7–10 MBq ^{18}F -FDG (GE Healthcare AS, Oslo, Norway) diluted in heparinised saline [7]. Acquisition of list-mode data started prior to ^{18}F -FDG injection and lasted for 50 minutes post-injection. The dynamic PET images were reconstructed using OSEM-MAP [16,17] producing images with a voxel size of $0.87 \times 0.87 \times 0.80 \text{ mm}^3$. The reconstructed time frames were 10 seconds during the initial 1.5 minutes followed by reduced temporal resolution for the remaining frames. Kinetic modeling of the DICOM-images was performed using in-house written IDL-programs (Interactive Data Language, v6.2, Research Systems Inc., Boulder, CO, USA). Briefly, the mean time activity curves (TACs) for each tumour were calculated and normalised to individual arterial input functions (AIFs) to account

for differences in the injected ^{18}F -FDG activity between the animals [9].

A three-compartment model consisting of a blood compartment and two sequential tissue compartments was used to evaluate the ^{18}F -FDG kinetics. The concentration in tissue (C_T) is assumed to be separated into a free (non-metabolised) and a bound (metabolised) compartment with tracer concentrations of C_F and C_B , respectively (Figure 1). The exchange of ^{18}F -FDG between the two tissue compartments is described by the rate constants k_1 , k_2 , k_3 , and k_4 [min^{-1}], where k_1 includes perfusion, vascular permeability and the binding of ^{18}F -FDG to the GLUT receptors, k_2 the clearance of ^{18}F -FDG back into the blood, k_3 the cellular internalisation, and k_4 the cellular externalisation. The kinetic parameters were estimated by fitting the TAC to this model and non-linear least squares minimisation. k_4 was assumed to be low, and was set to zero in the calculations. The blood volume fraction (v_B) was estimated as described previously [18]. The metabolic rate of ^{18}F -FDG (MR_{FDG}) was defined as $(k_1 \cdot k_3)/(k_2 + k_3)$. The fit between the measured TACs and the curves obtained from modeling were evaluated by calculating correction coefficients (r^2) for each tumour voxel.

Histopathology and immunohistochemistry

At the end of the experiment the mice were sacrificed by neck dislocation and tumour sites were matched with the in vivo imaging slices. The xenografts were excised and divided in two; one half was snap-frozen in liquid nitrogen and stored at -80°C , while the second half was formalin-fixed and paraffin-embedded.

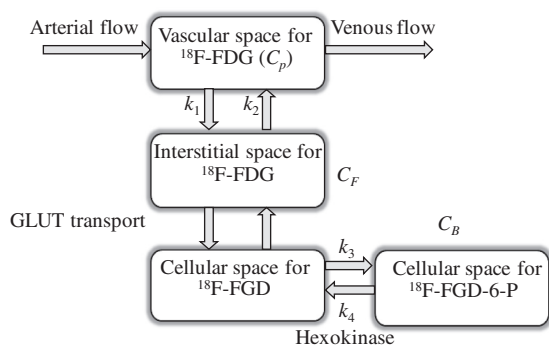


Figure 1. The three-compartment model used for extracting pharmacokinetic information from dynamic ^{18}F -FDG PET. C_p is the concentration of ^{18}F -FDG in plasma, and the tissue concentration C_T is composed of non-metabolized, or free, ^{18}F -FDG C_F , and metabolized, or bound, ^{18}F -FDG, C_B . C_T is further separated into not metabolised or free ^{18}F -FDG, C_F , and metabolised or bound ^{18}F -FDG, C_B . The kinetic parameters k_1 (min^{-1}) and k_2 (min^{-1}) describe the forward and backward ^{18}F -FDG diffusion, respectively. The k_3 (min^{-1}) and k_4 (min^{-1}) parameters signify the rates of ^{18}F -FDG phosphorylation and dephosphorylation, respectively, i.e., reflecting protein binding or glucose metabolism.

The paraffin-embedded sections were stained using a standard method (Dako EnVisionTM+ System, Peroxidase (DAB) (K4011, Dako, Glostrup, Denmark) and a Dako Autostainer). The primary antibodies, dilutions, pH retrieval solution and the positive controls are listed in Table I. The proportion of positively staining tumour cells was assessed semi-quantitatively as absent (0, no immunostaining), slight (1, $< 10\%$ of tumour cells were stained), moderate (2, $10\text{--}50\%$ of cells showed staining), or strong (3, $> 50\%$ of cells were stained). The intensity of staining was recorded as absent (0), weak (1), moderate (2) or strong (3). A staining score was obtained by multiplying these two values. The mitotic index was counted per 20 high power fields (HPFs) using a Leica DM2500 microscope (Leica Microsystems CMS, Germany) with an objective $\times 40$ giving an area of 0.31 mm^2 for a single HPF.

KIT and PDGFRA mutation analysis

Genomic DNA was extracted from 10 AHAX xenografts. Thirty nanograms of DNA was amplified using Phusion® Hot Start DNA polymerase and Phusion GC buffer (Finnzymes, Espoo, Finland). The thermal cycling conditions were DNA denaturation at 98°C for 30 seconds, five cycles at 98°C for 10 seconds, 65°C for 15 seconds and 72°C for 10 seconds, followed by 35 similar cycles where the annealing temperature was reduced to 60°C . Final extension was allowed at 72°C for 1 minute (The forward and reverse PCR primer pairs used can be provided upon request). The sequencing reactions were performed in two directions using the BigDye® Terminator v1.1 Cycle Sequencing Kit (Life Technologies, Carlsbad, CA, USA). The sequencing products were run on an automatic capillary sequencer (3130xl Genetic Analyzer, Life Technologies, Paisley, UK).

Statistical analysis

Statistical analyses were performed using Excel® (Microsoft Corporation, Redmond, WA, USA) and SPSS version 18.0 (SPSS Science, Chicago, IL, USA). Non-Gaussian distributions were compared using the non-parametric Mann-Whitney U-test. Two-sided t-test was used to compare the first order least-square linear regression estimated tumour doubling times. Significance was set to 5%.

Results

Tumour growth

Tumour growth was observed in 70 (95%) of the 74 implants in the 37 mice. One mouse was sacrificed prematurely because of oesophageal perforation and

Table I. The primary antibodies used for immunohistochemistry.

Antibody target	Company	Catalogue number	Dilution	Retrieval solution pH*	Positive control
GLUT-1	Abcam, Cambridge, UK	Ab652	1:200	Low pH	Kidney cancer
GLUT-2	Santa Cruz Biotechnology, Inc., Santa Cruz, CA, USA	Sc-9117	1:100	Low pH	Pancreas
GLUT-3	Abcam, Cambridge, UK	Ab53095	1:200	High pH	Testis
GLUT-4	AbD Serotec, Oxford, UK	4670-1704	1:1000	High pH	Salivary gland
HIF-1 α	Novus Biologicals, Cambridge, UK	NB100-499	1:300	High pH	Placenta
Caspase-3	Cell Signaling Technology, Danvers, MA, USA	9664	1:100	High pH	Large cell lymphoma

*Low pH: citrate buffer, pH 6.1 (K8005, Dako, Glostrup, Denmark). High pH: Tris/EDTA, pH 9 (K8004, Dako, Glostrup, Denmark).

was excluded from the study. The tumour volumes did not differ significantly between the three groups prior to therapy, with a median pretreatment tumour volume of 120 mm³ (range; 22–340 mm³, SE; \pm 73 mm³). The normalised tumour volume growth curves are shown in Figure 2. The tumour volume doubling time in the control group was 24.7 days (95% CI 21.9–28.4 days). The tumour doubling time was significantly shorter in the intermittent imatinib group (47.4 days; 95% CI 40.6–56.9 days) compared to the continuous group (130.9 days; 95% CI 84.2–293.5 days; $p < 0.001$). Both treatment groups showed significantly longer tumour volume doubling times compared to the untreated tumours ($p < 0.001$).

Dynamic ¹⁸F-FDG PET

¹⁸F-FDG PET of the treated animals was performed after 88 days of treatment, at a time point where both treatment groups were receiving imatinib. Figure 3A shows a series of ¹⁸F-FDG PET images demonstrating tracer uptake in a flank tumour in the continuous imatinib group. The TACs from the tumours treated with intermittent imatinib showed higher uptake and

reached a plateau earlier after tracer injection as compared to the tumours treated with continuous imatinib (25 minutes vs. 30 minutes, respectively). The median area under the normalised TAC curve was 20% higher for the intermittent group, albeit not significantly different ($p = 0.08$) (data not shown).

TACs of two voxels located at different sites within a continuous imatinib-treated xenograft are shown in Figure 3B. Using kinetic modeling, the TAC of the voxels were separated into free (not metabolised) and bound (metabolised) components. The goodness of fit between the measured TACs and the uptake curves obtained from modeling ranged from 0.91 to 0.98 with no significant differences between the two treatment groups. Mean k_1 , k_2 , k_3 , MR_{FDG} and v_B for both treatment groups are summarised in Table II. Significant differences were found for the kinetic parameters k_1 , k_3 and MR_{FDG} . The influx k_1 parameter was 32% higher in the intermittent group ($p = 0.01$), while k_3 and MR_{FDG} were 95% ($p = 0.01$) and 50% ($p = 0.03$) higher in the continuous treatment group, respectively. No significant correlations were found between the tumour volumes and the tumour pharmacokinetic parameters.

Tumour histology and immunohistochemistry

Microscopic examination of the haematoxylin stained tumour sections revealed no differences in tumour morphology between the three groups. However, the mitotic index was significantly higher in the control group (median; 13 mitoses/20 HPFs) as compared to the continuous and the intermittent group (both medians 4/20 HPFs, $p = 0.02$). The cytoplasmic GLUT-1 expression was significantly higher in the control group as compared to the intermittent group (median score 9 vs. 6; $p = 0.023$) and the continuous group (median score 6; $p = 0.009$). Both treatment groups had a significantly higher expression of cytoplasmic GLUT-2 (both median scores 9) than the control group (median score 3; $p < 0.001$). The expression of both the cytoplasmic and the membranous form of GLUT-3 were significantly higher ($p < 0.001$) in xenografts treated with intermittent

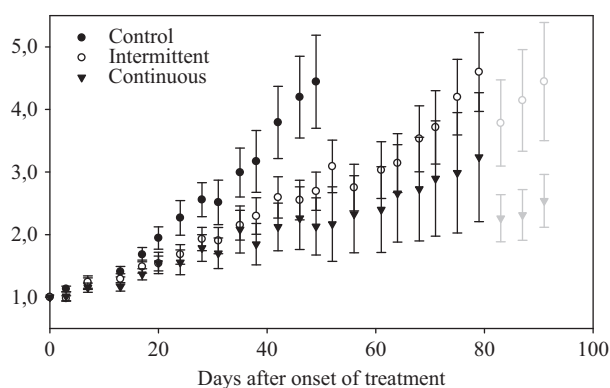


Figure 2. Normalised tumour volume growth of the human GIST AHAX xenograft in mice receiving either imatinib (100 mg/kg/day) continuously, intermittently (one week on, one week off) or placebo (water). At the end of experiment, mice with particularly large tumours were sacrificed, causing a dip in tumour volume growth (the light grey symbols). The data are given as means and standard errors of the means.

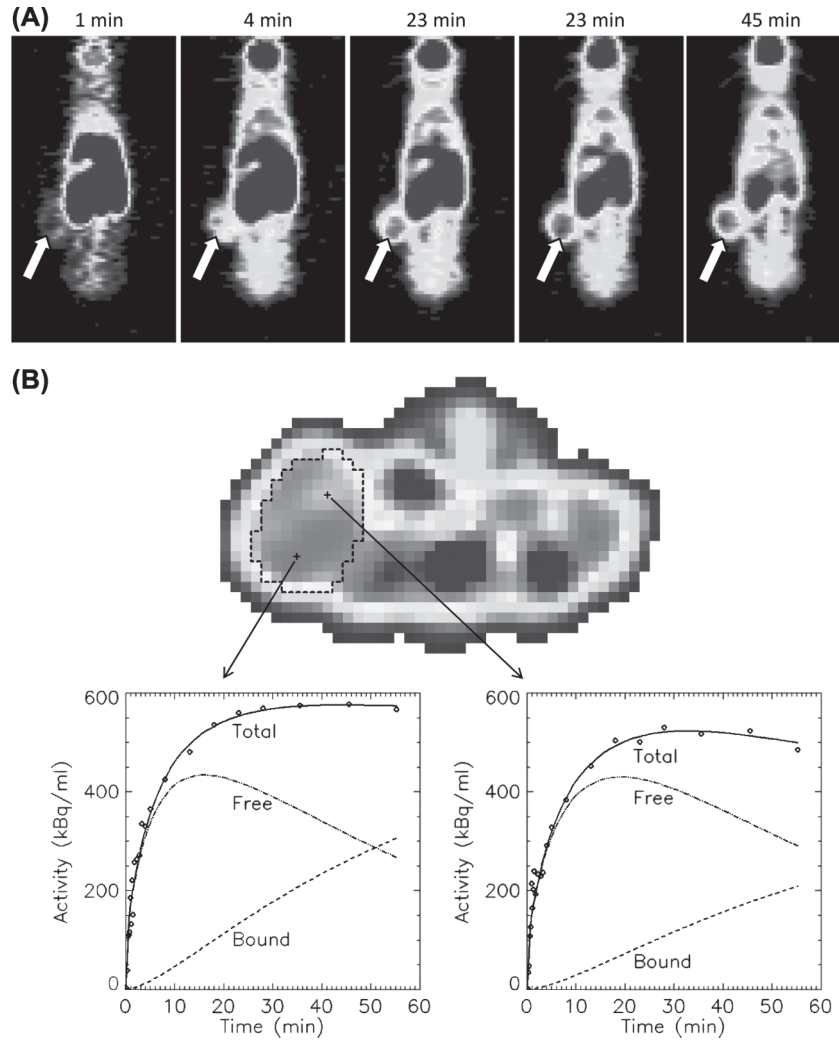


Figure 3. An example of cumulative ^{18}F -FDG uptake with time in a human GIST AHAX xenograft model (A). The white arrows point at the tumour. ^{18}F -FDG uptake as a function of time for two selected voxels within the xenograft is shown in (B). The uptake curves for the free and bound ^{18}F -FDG components obtained from kinetic modeling are provided.

imatinib (median score 3 and 3, respectively) as compared to xenografts treated with continuous imatinib (median score 0 and 0, respectively). There were no

Table II. Results from pharmacokinetic modelling of dynamic ^{18}F -FDG PET data. Data are given as median values.

Parameter	Treatment group		p*
	Intermittent imatinib	Continuous imatinib	
k_1 (min^{-1})	0.066	0.050	0.005
k_2 (min^{-1})	0.100	0.087	0.386
k_3 (min^{-1})	0.007	0.013	0.011
MR_{FDG} (min^{-1})	0.004	0.006	0.028
v_B	0.007	0.002	0.149

k_1 , k_2 and k_3 are the kinetic rate constants from the three-compartment model shown in Figure 1; MR_{FDG} the metabolic rate of ^{18}F -FDG; v_B , the estimated blood volume.

*p for the difference between the intermittent and continuous imatinib groups.

differences between the three groups with respect to HIF-1 α or caspase-3 expression (data not shown).

KIT and PDGFRA mutations

Ten xenografts (continuous group, 4; intermittent group, 3; control group, 3) were analysed for *KIT* and *PDGFRA* mutations to investigate tumour mutation status at the end of the experiment. Sequencing confirmed that all xenografts had maintained the original mutation in *KIT* exon 11 (c.1673_1687del, p.Lys558_Glu562del) and in *KIT* exon 17 (c.2446G>C, p.Asp816His). No further mutations were detected in *KIT* exons 9, 14 or 17, or in *PDGFRA* exons 12, 14 or 18.

Discussion

We explored the effects of imatinib administered either intermittently or continuously in a human

GIST xenograft harbouring the D816H mutation, which is a mutation considered to cause clinical imatinib resistance in GIST patients. The results show that the tumours do not regress either with intermittent or continuous imatinib, but, notably, they grow at a substantially slower rate than untreated tumours. This finding suggests that GISTs with a *KIT* 11 deletion mutation coupled with a D816H substitution mutation are not entirely imatinib-resistant. From a clinical point of view this is potentially an important observation, since the *KIT* exon 11 deletion mutation is the most common mutation in GIST, and exon 17 point mutations are the most frequent mutations considered to confer imatinib resistance. In clinical practice, imatinib administration is often discontinued when advanced GIST stops to respond to imatinib, and alternative treatments such as sunitinib or other TKIs are instituted. Anecdotal clinical experience suggests that reinstatement of imatinib after failure of the second- or third-line TKI treatments may still slow down GIST progression compared to no systemic treatment. Although firm clinical evidence is lacking, reinstatement of imatinib may still be advantageous as the last-line palliative care [12].

The reason for imatinib benefit in the presence of D816H remains hypothetical. The *KIT* exon 11 deletion mutation, unlike the D816H mutation, continues to be sensitive to imatinib, which may result in a less active KIT kinase in the presence of imatinib as compared to a kinase where both mutations are uninhibited. If this hypothesis is correct, the present findings may have relevance to many GISTs with an imatinib-sensitive primary mutation and an imatinib-insensitive secondary mutation. The original primary mutation is virtually always present in GISTs that contain a secondary resistance mutation [11]. Of note, more than one secondary mutation are commonly found in tumours that grow during imatinib treatment, sometimes even within the same metastasis [19]. Our findings may thus lend support to rechallenge with imatinib, even in cases when multiple secondary resistance mutations are present, provided that the primary mutation is imatinib-sensitive.

The French Sarcoma Group investigated in the randomised BRF14 trial the effect of interrupting imatinib treatment at after either one, three or five years of treatment in patients with advanced GIST who continued to respond to imatinib. Interruption of imatinib resulted in rapid GIST progression in the majority of patients, but almost all patients responded to imatinib reinstatement. No overall survival difference was seen between the interruption and the continuation groups, regardless of the timing of imatinib interruption [13,14]. Rapid cycling of imatinib administration (one week on, one week off) has not been tested in clinical trials, but the present result

showed no benefits during the 91-day observation period.

The AHAX xenograft model of human GIST has proven useful for studying ^{18}F -FDG uptake responses to TKIs [7]. In the current study we found differences in the dynamic ^{18}F -FDG uptake characteristics between the intermittent and the continuous treatment groups imaged while the mice were on imatinib. The TAC amplitude was higher in the intermittent group indicating either increased perfusion and/or increased metabolism compared to the continuous group. The tumour metabolic rate (MR_{FDG}), in turn, was higher in the continuous group, whereas k_1 was higher and k_3 lower in the intermittent group as compared to the continuous group suggesting presence of more perfusion, vascular permeability or vascular damage (high flow, leaky vessels) in the intermittent group [20]. Lack of correlations between tumour volumes and kinetic parameters indicate that tumour size could not explain the observed differences in FDG uptake. Taken together, these findings suggest that the schedule of imatinib administration influences tumour glucose uptake and metabolic rate. This observation should, however, be interpreted with some caution, since only four mice from each group underwent dynamic PET and the tumours showed heterogeneity in the PET parameters.

The GLUTs play a central role in the accumulation of ^{18}F -FDG within tumour cells. GLUT-1 is present in most cell types and is a key factor in glucose uptake, but different cancers express different GLUTs [21,22]. We found a difference in GLUT-3 expression between the two treatment groups. GLUT-3 is expressed in neurons and was originally designated as the neuronal GLUT. GISTs may show both muscle and neuronal differentiation and GLUT-3 expression may in part be related to rapid ^{18}F -FDG uptake in GISTs [23]. Imatinib induces GLUT translocation from the plasma membrane to the cytosol via endocytosis [24,25]. In line with this, we found higher cytoplasmic GLUT-2 expression in both imatinib groups compared to the control group.

In conclusion, the present study suggests that continuation of imatinib treatment may still benefit some GIST patients despite presence of an imatinib resistance mutation, such as D816H. In this setting, imatinib may slow down tumour progression, possibly by inhibiting the imatinib-sensitive primary mutation. Both continuous imatinib administration and the alternating one week on – one week off administration slowed down tumour progression, but the tumour growth was significantly more rapid with the alternating scheme. We found differences in ^{18}F -FDG uptake kinetics and tumour ^{18}F -FDG metabolic rate between the continuous and the intermittent imatinib

administration groups, but their clinical significance remains unknown.

Acknowledgements

The authors greatly acknowledge pathologist Ingvild Victoria Lobmaier and Bodil Bjerkehagen and the technical assistance provided by Mette Førsund and chief engineer Hong Qu.

Declaration of interest: The authors report no conflicts of interest. The authors alone are responsible for the content and writing of the paper.

This work was financially supported by the Norwegian Cancer Society grant 80114001 (TS) and The Norwegian Radium Hospital Research Foundation (MER).

References

- [1] Miettinen M, Lasota J. Gastrointestinal stromal tumors (GISTs): Definition, occurrence, pathology, differential diagnosis and molecular genetics. *Pol J Pathol* 2003;54:3–24.
- [2] Hirota S, Isozaki K, Moriyama Y, Hashimoto K, Nishida T, Ishiguro S, et al. Gain-of-function mutations of c-kit in human gastrointestinal stromal tumors. *Science* 1998;279:577–80.
- [3] Rubin BP, Singer S, Tsao C, Duensing A, Lux ML, Ruiz R, et al. KIT activation is a ubiquitous feature of gastrointestinal stromal tumors. *Cancer Res* 2001;61:8118–21.
- [4] Joensuu H, Roberts PJ, Sarlomo-Rikala M, Andersson LC, Tervahartiala P, Tuveson D, et al. Effect of the tyrosine kinase inhibitor STI571 in a patient with a metastatic gastrointestinal stromal tumor. *N Engl J Med* 2001;344:1052–6.
- [5] Blanke CD, Demetri GD, von MM, Heinrich MC, Eisenberg B, Fletcher JA, et al. Long-term results from a randomized phase II trial of standard versus higher-dose imatinib mesylate for patients with unresectable or metastatic gastrointestinal stromal tumors expressing KIT. *J Clin Oncol* 2008;26:620–5.
- [6] Gramza AW, Corless CL, Heinrich MC. Resistance to tyrosine kinase inhibitors in gastrointestinal stromal tumors. *Clin Cancer Res* 2009;15:7510–8.
- [7] Revheim ME, Roe K, Bruland OS, Bach-Gansmo T, Skretting A, Seierstad T. Monitoring the effect of targeted therapies in a gastrointestinal stromal tumor xenograft using a clinical PET/CT. *Mol Imaging Biol* 2011;13:1234–40.
- [8] Shinto A, Nair N, Dutt A, Baghel NS. Early response assessment in gastrointestinal stromal tumors with FDG PET scan 24 hours after a single dose of imatinib. *Clin Nucl Med* 2008;33:486–7.
- [9] Roe K, Aleksandersen TB, Kristian A, Nilsen LB, Seierstad T, Qu H, et al. Preclinical dynamic 18F-FDG. *Acta Oncol* 2010;49:914–21.
- [10] Revheim ME, Seierstad T, Berner JM, Bruland OS, Roe K, Ohnstad HO, et al. Establishment and characterization of a human gastrointestinal stromal tumour (GIST) xenograft in athymic nude mice. *Anticancer Res* 2009;29:4331–6.
- [11] Heinrich MC, Corless CL, Blanke CD, Demetri GD, Joensuu H, Roberts PJ, et al. Molecular correlates of imatinib resistance in gastrointestinal stromal tumors. *J Clin Oncol* 2006;24:4764–74.
- [12] National Comprehensive Cancer Network. Clinical practice guidelines in oncology. Soft tissue sarcoma. [2]. 2012. Ref Type: Data File.
- [13] Blay JY, Le CA, Ray-Coquard I, Bui B, Duffaud F, Delbaldo C, et al. Prospective multicentric randomized phase III study of imatinib in patients with advanced gastrointestinal stromal tumors comparing interruption versus continuation of treatment beyond 1 year: The French Sarcoma Group. *J Clin Oncol* 2007;25:1107–13.
- [14] Le CA, Ray-Coquard I, Bui BN, Adenis A, Rios M, Bertucci F, et al. Discontinuation of imatinib in patients with advanced gastrointestinal stromal tumours after 3 years of treatment: An open-label multicentre randomised phase 3 trial. *Lancet Oncol* 2010;11:942–9.
- [15] Euhus DM, Hudd C, LaRegina MC, Johnson FE. Tumor measurement in the nude mouse. *J Surg Oncol* 1986;31:229–34.
- [16] Qi J, Leahy RM, Cherry SR, Chatzioannou A, Farquhar TH. High-resolution 3D Bayesian image reconstruction using the microPET small-animal scanner. *Phys Med Biol* 1998;43:1001–13.
- [17] Qi J, Leahy RM. Resolution and noise properties of MAP reconstruction for fully 3-D PET. *IEEE Trans Med Imaging* 2000;19:493–506.
- [18] Kamasak ME, Bouman CA, Morris ED, Sauer K. Direct reconstruction of kinetic parameter images from dynamic PET data. *IEEE Trans Med Imaging* 2005;24:636–50.
- [19] Liegl B, Kepten I, Le C, Zhu M, Demetri GD, Heinrich MC, et al. Heterogeneity of kinase inhibitor resistance mechanisms in GIST. *J Pathol* 2008;216:64–74.
- [20] Mullani NA, Herbst RS, O'Neil RG, Gould KL, Barron BJ, Abbruzzese JL. Tumor blood flow measured by PET dynamic imaging of first-pass 18F-FDG uptake: A comparison with 15O-labeled water-measured blood flow. *J Nucl Med* 2008;49:517–23.
- [21] Godoy A, Ulloa V, Rodriguez F, Reinicke K, Yanez AJ, Garcia ML, et al. Differential subcellular distribution of glucose transporters GLUT1-6 and GLUT9 in human cancer: Ultrastructural localization of GLUT1 and GLUT5 in breast tumor tissues. *J Cell Physiol* 2006;207:614–27.
- [22] Yamamoto T, Seino Y, Fukumoto H, Koh G, Yano H, Inagaki N, et al. Over-expression of facilitative glucose transporter genes in human cancer. *Biochem Biophys Res Commun* 1990;170:223–30.
- [23] Gogvadze V, Orrenius S, Zhivotovsky B. Mitochondria in cancer cells: What is so special about them? *Trends Cell Biol* 2008;18:165–73.
- [24] Prenen H, Stefan C, Landuyt B, Vermaelen P, Debiec-Rychter M, Bollen M, et al. Imatinib mesylate inhibits glucose uptake in gastrointestinal stromal tumor cells by downregulation of the glucose transporters recruitment to the plasma membrane. *Am J Biochem Biotechnol* 2005;1:95–102.
- [25] Tarn C, Skorobogatko YV, Taguchi T, Eisenberg B, von MM, Godwin AK. Therapeutic effect of imatinib in gastrointestinal stromal tumors: AKT signaling dependent and independent mechanisms. *Cancer Res* 2006;66:5477–86.